Earthline Journal of Chemical Sciences
E-ISSN: 2581-9003; CODEN: EJCSB4
Volume 9, Number 2, 2023, Pages 209-226
https://doi.org/10.34198/ejcs.9223.209226

Some Tautomers of Amrinone and their Interaction with Calcium Cation - DFT Treatment

Lemi Türker

Department of Chemistry, Middle East Technical University, Üniversiteler, Eskişehir Yolu No: 1, 06800 Çankaya/Ankara, Turkey; e-mail: lturker@gmail.com; lturker@metu.edu.tr

Abstract

Amrinone, is a pyridine phosphodiesterase 3 inhibitor. It is prescribed to patients suffering from congestive heart failure. In the present study, amrinone and it tautomers have been studied computationally within the limitations of the density functional theory and the basis set employed (B3LYP/6-31++G(d,p)). The calculations have also been extended to interaction of those tautomers with calcium cation. All the tautomers and their composites with the calcium cation are electronically and structurally stable. Some quantum chemical and spectral properties of those systems have been obtained and discussed.

1. Introduction

Amrinone, chemically is a lactam, also known as inamrinone, and sold on the market as inocor. It is a pyridine phosphodiesterase 3 inhibitor [1] which is a drug that may improve the prognosis in patients suffering from congestive heart failure [2]. Medicinally amrinone has been shown to increase the contractions initiated in the heart by high-gain calcium induced calcium release (CICR) [3]. Its mode of action occurs by inhibiting the breakdown of both cAMP and cGMP by the phosphodiesterase (PDE3) enzyme. Consequently, an increase in level of cAMP with the administration of amrinone in vascular smooth muscle produces vasodilatation by facilitating calcium uptake by the sarcoplasmic reticulum and decreasing the calcium available for contraction [4,5]. In myocytes, it has been shown that the increase of cAMP concentration increases in turn the activity of PKA thus this kinase improves the inward Ca^{2+} current through the L-type

Received: November 8, 2022; Accepted: December 5, 2022; Published: December 7, 2022

Keywords and phrases: amrinone; inamrinone; inocor; tautomers; DFT.

Ca^{2+} channels. Hence, it leads to calcium-induced calcium release from the sarcoplasmic reticulum, giving rise to a calcium spark that triggers the contraction; this results in an inotropic effect. In man the primary route of excretion of both inamrinone and its several metabolites (N-glycolyl, N-acetate, O-glucuronide and N-glucuronide) is via the urinary system.

Innumerous articles are present in the literature about the medicinal aspects of amrinone. Comparatively only a few articles exist about modeling studies [6] and theoretical calculations [7]. However, in recent years some attention has been focused on the conformations of bipyridine cardiotonics on account of their potential inotropic and peripheral vasodilatory properties [8-10]. Although several experimental studies [11,12] (Suzuki and Lambert et al.,) have been made earlier in order to rationalize the conformational changes on the basis of crystal forces, little work has been done to support the experimental observations with theoretical conformational analysis which might help to reveal the important structural prerequisites for understanding the structure-activity relations. Conformational features of amrinone and its analogue milrinone have been examined via *ab initio* (at STO-3G and 3-21G levels) molecular orbital theory [13]. The computational results of this theoretical investigation clearly have indicated that amrinone possesses much greater flexibility when compared with that of milrinone. Hence, greater cardiotonic potency of milrinone is most likely due to the reduced conformational flexibility because of the existing 2-methyl group.

On the other hand, it is known that tautomers having different structures possess dual reactivity, therefore it is anticipated that a material which is potent to exhibit tautomerism should display variable properties depending on its tautomer content (allelotropic mixture [14]). It is worth noting that substances which are isomeric under certain conditions are tautomeric under more drastic conditions [14]. Therefore, it would be interesting to put some light on to the tautomerism of amrinone. In the present study not only the tautomerism exhibited by amrinone but also the interactions of amrinone and some of its tautomers with calcium cation have been investigated within the limitations of the density functional theory (DFT) and the basis set employed.

2. Method of Calculations

All the structures presently considered have been subjected to the geometry optimizations leading to energy minima. The optimizations have been achieved first by using MM2 method which is followed by semi-empirical PM3 self consistent fields

molecular orbital (SCF MO) method [15,16] (at the restricted level [17,18]). Subsequent optimizations have been performed at Hartree-Fock level employing sequentially various basis sets. Afterwards, geometry optimizations were managed within the framework of density functional theory [19,20] at the level of B3LYP/6-31++G(d,p) [17,21]. Note that the exchange term of B3LYP consists of hybrid Hartree-Fock and local spin density (LSD) exchange functions with Becke's gradient correlation to LSD exchange [20,22]. The correlation term of B3LYP consists of the Vosko, Wilk, Nusair (VWN3) local correlation functional [23] and Lee, Yang, Parr (LYP) correlation correction functional [24]. Also, additionally vibrational analyses have been done on the optimized structures. The total electronic energies are corrected for the zero point vibrational energy (ZPE). Moreover, the normal mode analysis for each structure yielded no imaginary frequencies for the $3N–6$ vibrational degrees of freedom, where N stands for the number of atoms in the each system considered. Thus it has been indicated that the structure of each molecule corresponds to at least a local minimum on the potential energy surface. All these calculations have been done by using the Spartan 06 package program [25]. Whereas the nucleus-independent chemical shift (NICS(0)) calculations have been performed by using Gaussian 03 program [26].

3. Results and Discussion

It would be interesting to investigate the tautomers of amrinone and then their interactions with calcium cation because amrinone increases the contractions initiated in the heart by high-gain calcium induced calcium release process.

Figure 1 shows amrinone (A) and its 1,3- and 1,7-type tautomers (structures B and C, respectively). Note that amrinone possesses a lactam whereas its 1,3-tautomer has an

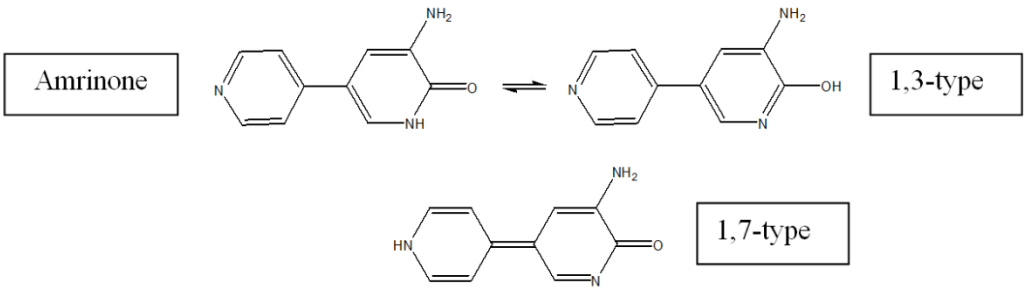

Figure 1. Amrinone and its 1,3- and 1,7-type tautomers.

embedded lactim system. Their optimized structures are included in Figure 2. As seen in the figure in 1.7-type tautomer the rings are coplanar with each other and there exists no aromatic ring. In tautomers A and B the rings possess certain degree of twist angle. However it is worth mentioning that in general 1,7-type tautomers have less likely occurrence as compared to 1,3- and 1,5-types.

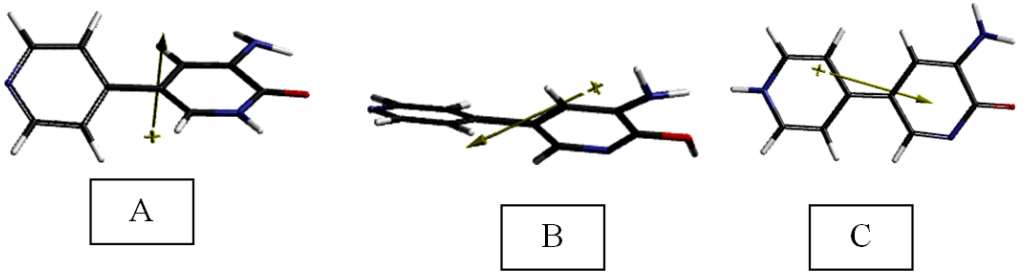

Figure 2. Optimized structures of the tautomers considered.

Table 1 lists some properties of the tautomers considered. Tautomer-C, differs distinctly from the others in terms of the dipole moment and logP values. The dipole moment vector of tautomer-C originates from 1,4-dihydropyridine like ring to the lactam ring (see Figure 3) which is opposite to the direction of the vector in tautomer-B. Whereas in amrinone the dipole moment vector is almost perpendicular to the lactam ring. Note that tautomer-C has the lowest logP value and hydrophilic drugs (having low octanol/water partition coefficients) are found primarily in aqueous regions. Considering this fact together with its high dipole moment value structure of tautomer-C should be highly polar one.

Table 1. Some properties of the tautomers considered.

Tautomer	logP	Dipole moment	Polarizability	Ovality
A	-1.57	0.71	55.62	1.30
B	-0.70	3.28	55.53	1.30
C	-2.01	13.40	55.97	1.29

Dipole moments in debye units. Polarizabilities in 10^{-30} m^3 units.

Figure 3 shows the electrostatic potential (ESP) charges on the atoms of the tautomers considered. It is worth noting that the ESP charges are obtained by the program based on a numerical method that generates charges that reproduce the electrostatic potential field from the entire wavefunction [25].

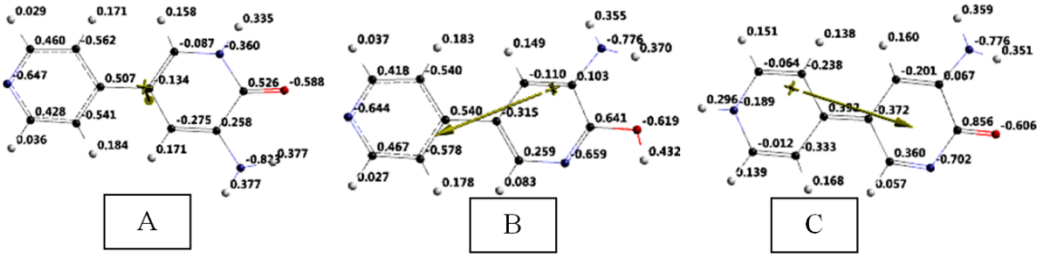

Figure 3. The ESP charges on the atoms of the tautomers considered.

Table 2 shows some energies of the tautomers considered, where E, ZPE and E_C stand for the total electronic energy, zero point vibrational energy and the corrected total electronic energy, respectively. The data reveal that all the structures considered are electronically stable. The E_C values follow the order of A<B<C, thus A and C are electronically the most and least stable tautomers, respectively.

Table 2. Some energies of the tautomers considered.

Tautomer	E	ZPE	E_C
A	-1643613.24	471.44	-1643141.80
B	-1643599.20	471.04	-1643128.16
C	-1643506.00	468.45	-1643037.55

Energies in kJ/mol.

In Table 3 aqueous energies of the tautomers are listed. The same order of stability is valid in aqueous conditions as in the vacuum.

Table 3. Aqueous energies of the tautomers considered.

A	B	C
-1643674.84	-1643660.51	-1643643.02

Energies in kJ/mol.

Table 4 tabulates some calculated stretching frequencies of the tautomers.

Table 4. Some calculated stretching frequencies of the tautomers.

Frequency	A	B	C
N-H	3707, 4570	3691,3577	3660(NH), 3552(NH_2)
O-H		3788	
C=O	1727		1682

Frequencies in cm^{-1}

Some thermo chemical values for the tautomers are listed in Table 5. As seen in the table they all have exothermic heat of formation values and favorable Gº values. Tautomer-A is the most exothermic and the most favorable one in the group.

Table 5. Some energies of the tautomers considered.

Tautomer	Hº	Sº (J/molº)	Gº
A	-1643128.079	408.56	-1643249.890
B	-1643114.405	408.42	-1643236.177
C	-1643023.213	412.02	-1643146.059

Energies in kJ/mol.

Figure 4 displays some of the molecular orbital energies of the tautomers. As seen in the figure the HOMO and LUMO energies decrease as going from tautomer-A to B. Note that in tautomer-B a new aromatic ring emerges at an expense of the lactam ring. Although the rings are not coplanar there exists some partial conjugation in between them. In addition the amino and hydroxyl groups (which are both electron donor substituents) interfere with the conjugation causing the HOMO and LUMO energies decrease. Note that the inner lying molecular orbitals are also perturbed in terms of energy in going from tautomer-A to B. As for tautomer-C, prevailing conjugative effects raise the HOMO but lower the LUMO energies as compared to the others.

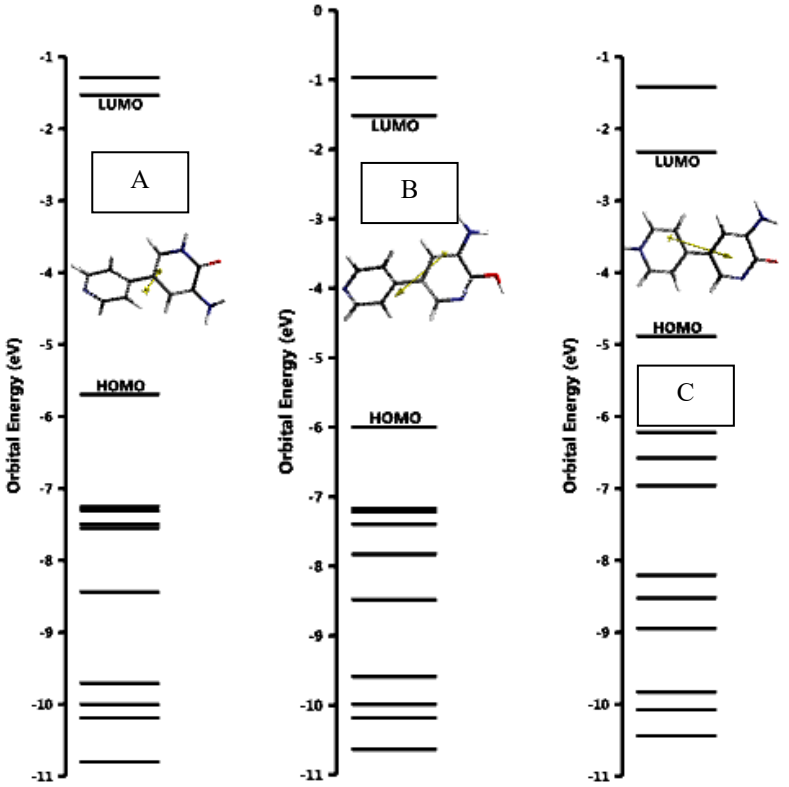

Figure 4. Some of the molecular orbital energies of the tautomers.

Table 6 lists the HOMO and LUMO energies as well as the interfrontier molecular orbital energy gaps ($\Delta\varepsilon$, $\Delta\varepsilon = \varepsilon_{LUMO}-\varepsilon_{HOMO}$) of the tautomers considered. The orders of the HOMO and LUMO energies are B<A<C and C<A<B, respectively. Note that in tautomer-A some sort of extended conjugation exists in the lactam ring which is exchanged with some other sort of extended conjugation (aromatic ring emerges) in tautomer-B. Additionally in B the amino and hydroxyl substituents are oriented in such a way that their similar type inductive and mesomeric effects are opposing to each other on the aromatic ring. These perplexing interactions causes the present situations to arise in the HOMO and LUMO energies of tautomers A and B. Tautomer-C is different from the others because two rings in its structure are coplanar, thus a long extended conjugation exists to raise the HOMO but lower the LUMO energy[27]. Whereas $\Delta\varepsilon$ values follow the order of C<A<B. The consequence of this order (narrowing interfrontier molecular orbital gap) is reflected in the UV-VIS spectra (time dependent DFT spectra) as seen in

Figure 5. There, tautomer-C having the smallest interfrontier molecular orbital energy gap exhibits a striking bathochromic effect as compared to the others.

Table 6. The HOMO and LUMO energies and Δε values of the tautomers considered.

Tautomer	HOMO	LUMO	Δε
A	-549.46	-147.85	401.61
B	-579.03	-146.55	432.48
C	-471.51	-224.53	246.98

Energies in kJ/mol.

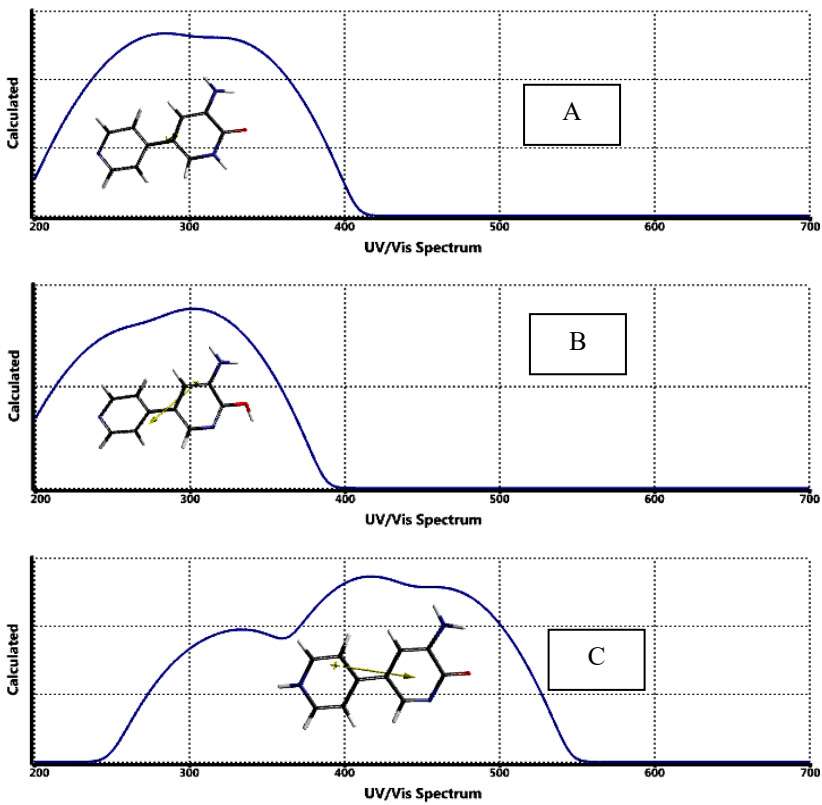

Figure 5. UV-VIS spectra of the tautomers.

Figure 6 shows the variation of the HOMO and LUMO patterns from tautomer to tautomer. They mostly exhibit π-type symmetry. In tautomers A and B, mainly the lactam or lactim ring contributes into the HOMO. Whereas in tautomer-C the pyridyl ring also contributes quite appreciably into the HOMO. In the case of the LUMO both of the rings are the contributors.

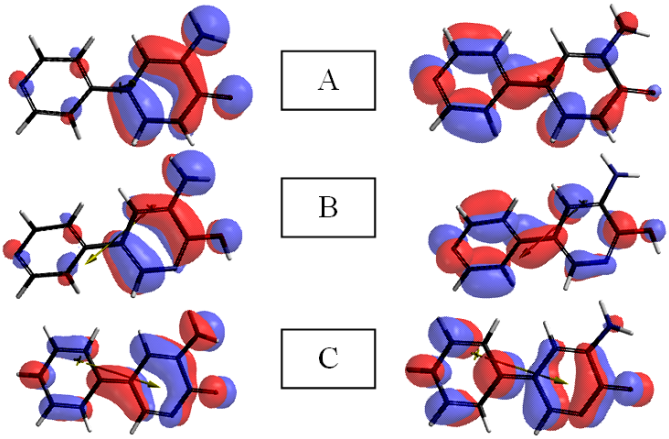

Figure 6. Variation of the HOMO and LUMO patterns of the tautomers.

Figure 7 displays the local ionization maps of the tautomers. Note that conventionally red/reddish regions (if any exists) on the density surface indicate areas from which electron removal is relatively easy, meaning that they are subject to electrophilic attack.

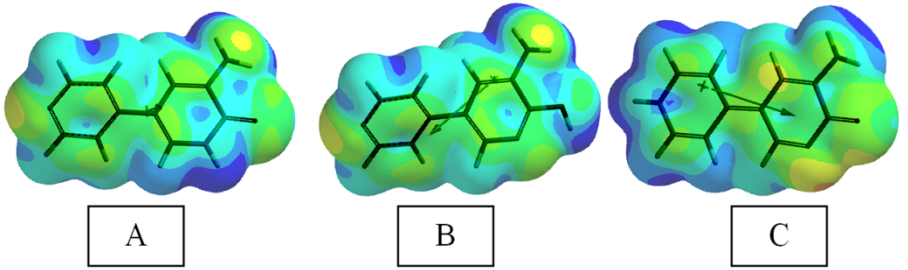

Figure 7. Local ionization maps of the tautomers.

Figure 8 displays the LUMO maps of the tautomers. A LUMO map displays the absolute value of the LUMO on the electron density surface. The blue color (if any exists) stands for the maximum value of the LUMO and the red colored region, associates with the minimum value.

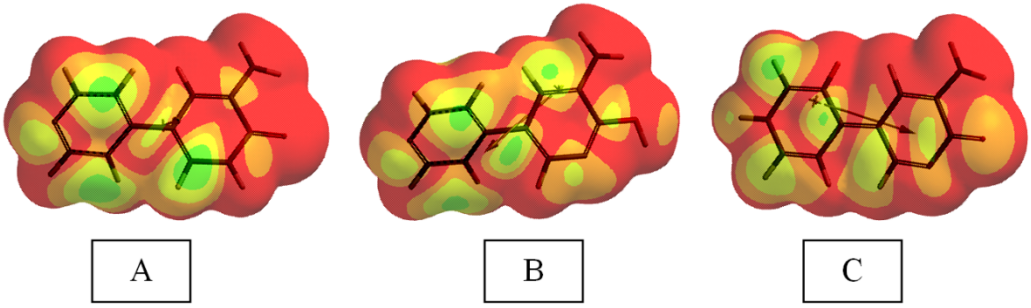

Figure 8. The LUMO maps of the tautomers.

NICS

Table 7 tabulates "nucleus-independent chemical shift" (NICS) values of amrinone and its 1,3-and 1,7-type tautomers considered, where A1 and B1 stand for the pyridyl ring in tautomers A and B, respectively whereas B2 stands for the ring having the embedded lactim moiety in tautomer-B. NICS is the computed value of the negative magnetic shielding at some selected point in space. Generally it is calculated at center of a ring or cage (NICS(0)). Numerous articles have appeared in the literature during the last decades, discussing aromaticity in terms of energetic, structural and magnetic criteria [28-39]. Note that negative NICS values denote aromaticity (such as -11.5 for benzene, -11.4 for naphthalene). On the contrary, positive NICS values stand for antiaromaticity (28.8 for cyclobutadiene) while small NICS values are associated with non-aromaticity (-2.1 for cyclohexane, -1.1 for adamantine). However, it is to be mentioned that although NICS approach has been proved to be an effective probe for the local aromaticity of individual rings of polycyclic systems, a couple of contradictory results exist [39]. As seen in the table, the pyridyl ring of tautomer-A is more aromatic than the respective ring of B (as an approximation) and the ring possessing the embedded lactim group of B is more aromatic than its pyridyl ring. Note that the topology of the pyridyl ring in tautomer A and B is almost the same but the conjugation with the other ring is somewhat different (see Figure 2). The pyridyl ring of A is comparatively less conjugated with its lactam ring. All these variations in NICS values should arise from the topology of the rings and substituent effects acting on the ring current which is one of the main factors on the value of NICS.

Table 7. NICS(0) values of amrinone tautomers considered.

A1	B1	B2
-6.4672	-6.3223	-7.7338

Interaction with calcium cation

Figure 9 shows the optimized structures as well as the direction of the dipole moment vectors of the tautomer+Ca^{+2} composite species. The conformation of NH_2 substituent in A and B cases is such that the lone pair of it is next to the calcium cation. As compared to the parent tautomers, the presence of the calcium cation changes not only the directions of the dipole moment vectors but also the magnitudes of them (see Figure 2 and Table 1) which are 34.18, 38.63 and 15.69 debye, respectively for the tautomer+Ca^{+2} type species shown in Figure 9. Thus the order of the dipole moments in the presence of calcium cation is B+Ca^{+2}>A+Ca^{+2}>C+Ca^{+2}. Note that the order of dipole moments is C>B>A for the parent tautomers. The change of order should be due to the structural changes and distribution of the electrons affected by the presence of the cation.

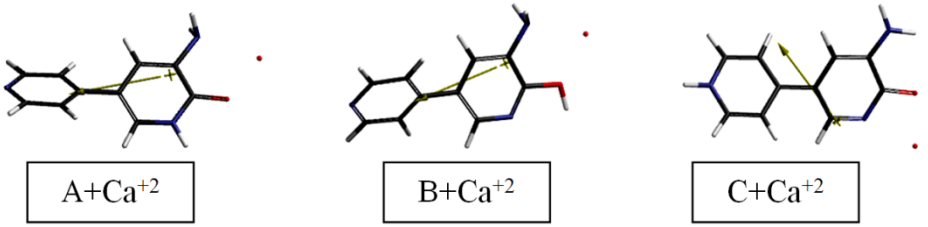

Figure 9. The optimized structures of the tautomer+Ca^{+2} species.

Figure 10 displays the ESP charges on the atoms of the tautomer+Ca^{+2} type species considered. As seen in the figure the charge on the calcium cation follows the order of B+Ca^{+2}>A+Ca^{+2}>C+Ca^{+2} which is the order of the dipole moments. It seems some electron population has been transferred from the organic part to the calcium cation in all three cases decreasing the original charge of the cation.

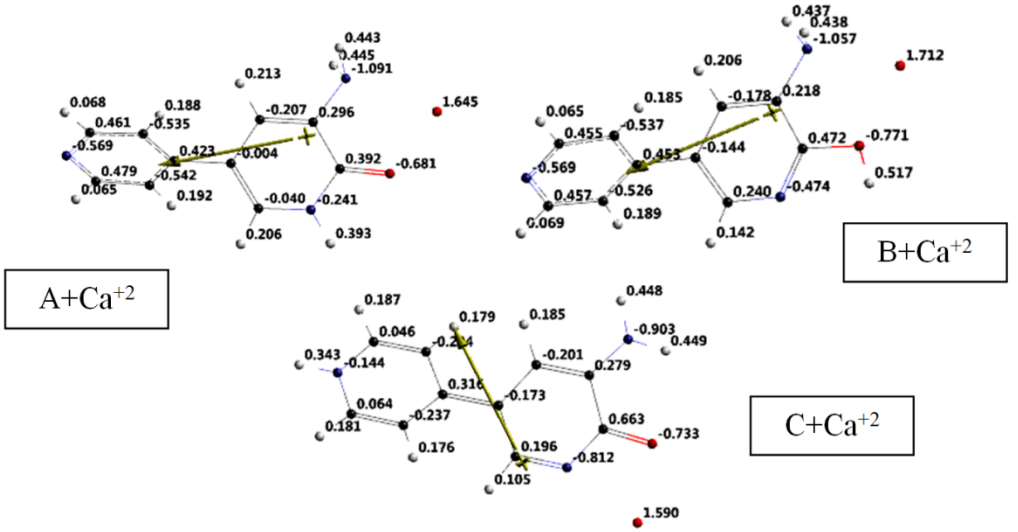

Figure 10. The ESP charges on the atoms of the tautomer+Ca^{+2} species considered.

Table 8 shows some energies of the tautomer+Ca^{+2} type species considered. According to the data presented, the electronic stabilities based on E_C values is C+Ca^{+2}> A+Ca^{+2}>B+Ca^{+2}. Note that the stability order for the parent tautomers is A>B>C (Table 2). The electronic stability arises from various factors which are implicit functions of each other, such as charge-charge, dipole-charge and dipole-dipole interactions (or more).

Table 8. Some energies of the tautomer+Ca^{+2} species considered.

Tautomer	E	ZPE	E_C
A+Ca^{+2}	-3421313.46	478.91	-3420834.55
B+Ca^{+2}	-3421165.78	474.98	-3420690.80
C+Ca^{+2}	-3421433.28	478.21	-3420955.07

Energies in kJ/mol.

Table 9 shows the HOMO, LUMO energies and Δε values of the tautomer+Ca^{+2} species considered. The orders of the HOMO and LUMO energies are A+Ca^{+2} < B+Ca^{+2} < C+Ca^{+2} and B+Ca^{+2} < A+Ca^{+2} < C+Ca^{+2}, respectively. Whereas the Δε values follow the order of C+Ca^{+2} > A+Ca^{+2} > B+Ca^{+2}.

Table 9. Some energies of the tautomer+Ca^{+2} species considered.

Tautomer	HOMO	LUMO	Δε
A+Ca^{+2}	-1152.31	-953.71	198.6
B+Ca^{+2}	-1128.29	-1039.56	88.73
C+Ca^{+2}	-1124.70	-850.75	273.95

Energies in kJ/mol.

Figure 11 shows some of the molecular orbital energy levels of amrinone and its 1,3-tautomer as well as the respective levels of the composites considered. As seen in the figure the cation affects not only the frontier molecular orbital energies but the inner lying ones as well.

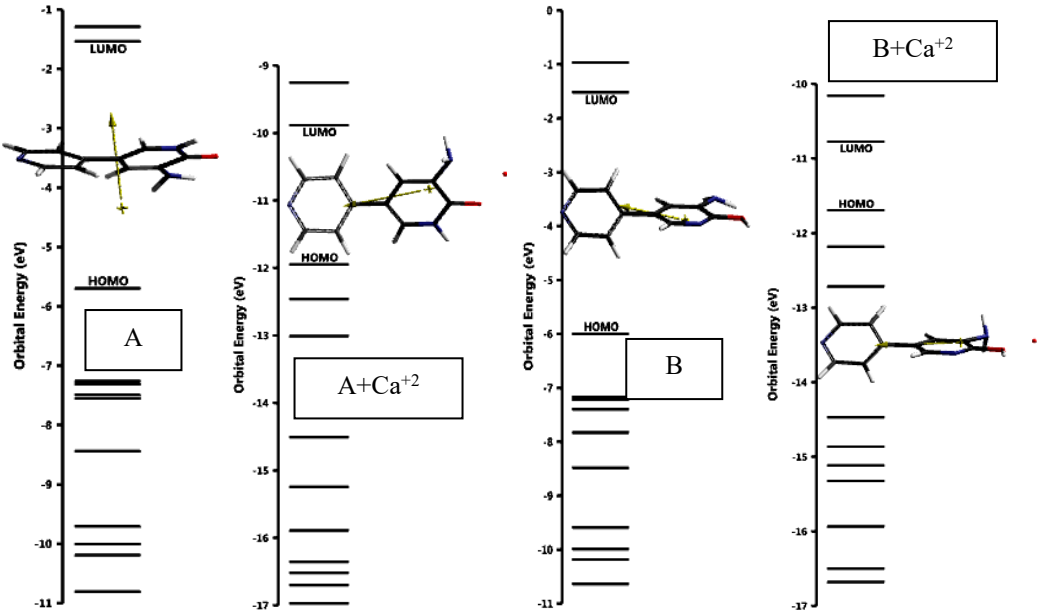

Figure 11. Some of the molecular orbital energy levels of amrinone, its 1,3-tautomer and their calcium cation composites.

The less likely tautomer C (1,7-type tautomer) and its composite are not shown in the figure.

The calculated time-dependent DFT UV-VIS spectra of A+Ca^{+2} and C+Ca^{+2} are shown in Figure 12, whereas B+Ca^{+2} spectrum due to bathochromic effect is out of scale of wavelengths.

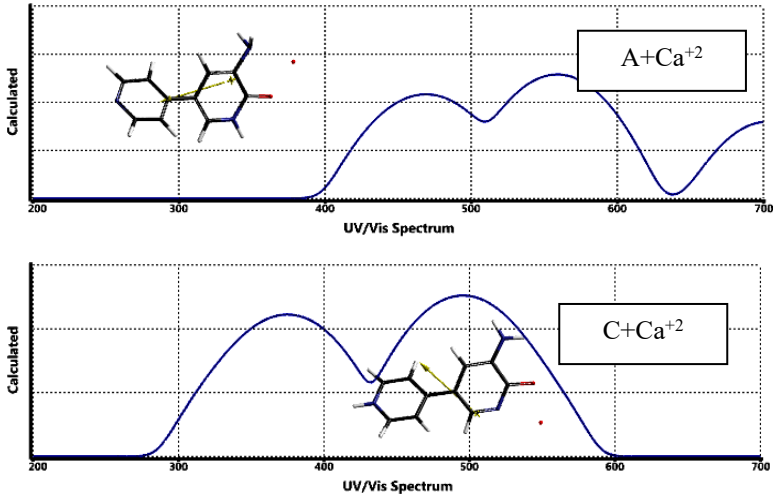

Figure 12. The calculated UV-VIS spectra.

Figure 13 shows the HOMO and LUMO patterns of the tautomer+Ca^{+2} species considered. As seen in the figure, in the cases of A+Ca^{+2} and B+Ca^{+2}, the HOMO has been confined to the pyridyl moiety whereas the LUMO is supplied mainly by the calcium cation. In the case of C+Ca^{+2} the HOMO is spread over the amino substituted ring which has little contribution to the LUMO. As compared to the HOMO and LUMO patterns of the parent tautomers (see Figure 6) it is evident that the calcium cation highly perturbs the patterns.

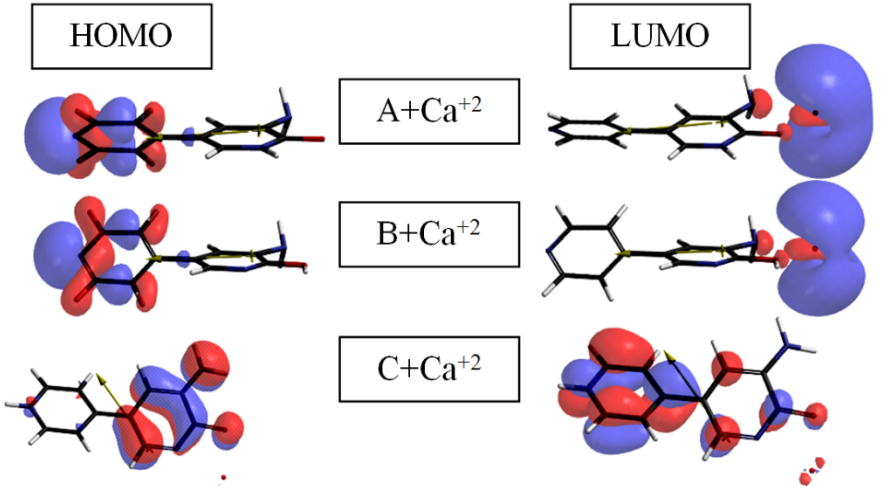

Figure 13. The HOMO and LUMO patterns of the tautomer+Ca^{+2} species considered.

4. Conclusion

The present density functional treatment, within the constraints of the theory and the basis set employed, has indicated that the positional variations of tautomeric hydrogen in amrinone results electronically stable and thermodynamically favorable tautomeric structures. However, 1,7-tautomer is rather different from the others, namely amrinone and its 1,3-tautomer. 1,7-Tautomer has the highest dipole moment and higher polarizability of the all. Also its interfrontier molecular orbital energy gap value is the smallest one, thus its UV-VIS spectrum is characterized with a bathochromic effect. The calculations have also been extended to interaction of those tautomers with the calcium cation. In each case, the composites are found to be stable. The cation highly perturbs the parent systems in terms of the energies, charge distributions and the molecular orbitals. In every case, some electron population has been transferred from the organic component to the cation by diminishing its positive charge. Thus, the observed medicinal effect of amrinone should be the result of over all effect with its tautomers and their interactions with the calcium cation.

References

[1] Hamada, Y., Kawachi, K., Yamamoto, T., Nakata, T., Kashu, Y., Sato, M., & Watanabe, Y. (1999). Effects of single administration of a phosphodiesterase III inhibitor during cardiopulmonary bypass: comparison of milrinone and amrinone. *Japanese Circulation Journal*, *63*(8), 605-9. https://doi.org/10.1253/jcj.63.605

[2] Klein, N.A., Siskind, S.J., Frishman, W.H., Sonnelblick, E.H., & LeJemtel, T.H. (1981). Hemodynamic comparison of intravenous amrinone and dobutamine in patients with chronic congestive heart failure. *American Journal of Cardiology*, *48*(1), 170-175. https://doi.org/10.1016/0002-9149(81)90587-7

[3] Xiong, W., Ferrier, G.R., & Howlett, S.E. (2004). Diminished inotropic response to amrinone in ventricular myocytes from myopathic hamsters is linked to depression of high-gain Ca^{2+}-induced Ca^{2+} release. *The Journal of Pharmacology and Experimental Therapeutics*, *310*(2), 761-773. https://doi.org/10.1124/jpet.103.064873

[4] Levy, J.H., Ramsay, J., & Bailey, J.M. (1990). Pharmacokinetics and pharmacodynamics of phosphodiesterase-III inhibitors. *Journal of Cardiothoracic Anesthesia*, *4*, 7-11. https://doi.org/10.1016/0888-6296(90)90226-6

[5] Packer, M., Medina, N., & Yushak, M. (1984). Hemodynamic and clinical limitations of long-term inotropic therapy with amrinone in patients with severe chronic heart failure. *Circulation*, *70*(6), 1038-1047. https://doi.org/10.1161/01.cir.70.6.1038

[6] Akcan, A., Kucuk, C., Ok, E., Canoz, O., Muhtaroglu, S., Yilmaz, N., & Yilmaz, Z. (2006). The effect of amrinone on liver regeneration in experimental hepatic resection model 1. *Journal of Surgical Research*, *130*(1), 66-72. https://doi.org/10.1016/j.jss.2005.07.020

[7] Chen, J., Zhao, H., Farajtabar, A., Zhu, P., Jouyban, A., & Acree, W.E. (2022). Equilibrium solubility of amrinone in aqueous co-solvent solutions reconsidered: Quantitative molecular surface, inter/intra-molecular interactions and solvation thermodynamics analysis. *Journal of Molecular Liquids*, *355*, 118995. https://doi.org/10.1016/j.molliq.2022.118995

[8] Miller, R.P., Palomo, A.R., Brandon, B.S., Hartley, C.J., & Quinones, M.A. (1981). Combined vasodilator and inotropic therapy of heart failure: Experimental and clinical concepts. *Am. Heart J.*, *102*, 500-508. https://doi.org/10.1016/0002-8703(81)90738-9

[9] Taylor, S.H., Silke, B., & Nelson, G.I.C. (1982). Principles of treatment of left ventricular failure. *Eur. Heart J.*, *3*, 19, Suppl D:19-43.

[10] Ward, A., Brogden, R.N., Heel, R.C., Speight, T.M., & Avery, G.S. (1983). A preliminary review of its pharmacological properties and therapeutic use. *Drugs*, *26*, 468-502. https://doi.org/10.2165/00003495-198326060-00002

[11] Suzuki, H. (1967). *Electronic absorption spectra and geometry of organic molecules.* New York: Academic Press.

[12] Lambert, J.B., Shurvell, H.F., Verbit, L., Cooks, R.G., & Stout, G.H. (1976). *Organic structural analysis*. New York: MacMillan.

[13] Bhattacharjee, A.K. (1990). Theoretical conformational study of the molecular structures of some bipyridine cardiotonics. *Proc. Indian Acad. Sci.* (*Chem. Sci.*), *102*, 159-163. https://doi.org/10.1007/bf02860153

[14] Reutov, O. (1970). *Theoretical principles of organic chemistry*. Moscow: Mir Pub.

[15] Stewart, J.J.P. (1989). Optimization of parameters for semi empirical methods I. Method. *J. Comput. Chem*., *10*, 209-220. https://doi.org/10.1002/jcc.540100208

[16] Stewart, J.J.P. (1989). Optimization of parameters for semi empirical methods II. Application. *J. Comput. Chem*., *10*, 221-264. https://doi.org/10.1002/jcc.540100209

[17] Leach, A.R. (1997). *Molecular modeling*. Essex: Longman.

[18] Fletcher, P. (1990). *Practical methods of optimization*. New York: Wiley.

[19] Kohn, W., & Sham, L. (1965). Self-consistent equations including exchange and correlation effects. *J. Phys. Rev.*, *140*, A1133-A1138. https://doi.org/10.1103/physrev.140.a1133

[20] Parr, R.G., & Yang, W. (1989). *Density functional theory of atoms and molecules*. London: Oxford University Press.

[21] Cramer, C.J. (2004). *Essentials of computational chemistry*. Chichester, West Sussex: Wiley.

[22] Becke, A.D. (1988). Density-functional exchange-energy approximation with correct asymptotic behavior. *Phys. Rev. A*, *38*, 3098-3100. https://doi.org/10.1103/physreva.38.3098

[23] Vosko, S.H., Wilk, L., & Nusair, M. (1980). Accurate spin-dependent electron liquid correlation energies for local spin density calculations: a critical analysis. *Can. J. Phys.*, *58*, 1200-1211. https://doi.org/10.1139/p80-159

[24] Lee, C., Yang, W., & Parr, R.G. (1988). Development of the Colle-Salvetti correlation energy formula into a functional of the electron density. *Phys. Rev. B*, *37*, 785-789. https://doi.org/10.1103/physrevb.37.785

[25] SPARTAN 06 (2006). Wavefunction Inc., Irvine CA, USA.

[26] Gaussian 03 (2004). Frisch, M.J., Trucks, G.W., Schlegel, H.B., Scuseria, G.E., Robb, M.A., Cheeseman, J.R., Montgomery, Jr., J.A., Vreven, T., Kudin, K.N., Burant, J.C., Millam, J.M., Iyengar, S.S., Tomasi, J., Barone, V., Mennucci, B., Cossi, M., Scalmani, G., Rega, N., Petersson, G.A., Nakatsuji, H., Hada, M., Ehara, M., Toyota, K., Fukuda, R., Hasegawa, J., Ishida, M., Nakajima, T., Honda, Y., Kitao, O., Nakai, H., Klene, M., Li, X., Knox, J.E., Hratchian, H.P., Cross, J.B., Bakken, V., Adamo, C., Jaramillo, J., Gomperts, R., Stratmann, R.E., Yazyev, O., Austin, A.J., Cammi, R., Pomelli, C., Ochterski, J.W., Ayala, P.Y., Morokuma, K., Voth, G.A., Salvador, P., Dannenberg, J. J., Zakrzewski, V.G., Dapprich, S., Daniels, A.D., Strain, M.C., Farkas, O., Malick, D. K., Rabuck, A.D., Raghavachari, K., Foresman, J.B., Ortiz, J.V., Cui, Q., Baboul, A.G., Clifford, S., Cioslowski, J., Stefanov, B.B., Liu, G., Liashenko, A., Piskorz, P., Komaromi, I., Martin, R.L., Fox, D.J., Keith, T., Al-Laham, M.A., Peng, C.Y., Nanayakkara, A., Challacombe, M., Gill, P.M.W., Johnson, B., Chen, W., Wong, M. W., Gonzalez, C., & Pople, J.A., Gaussian, Inc., Wallingford CT.

[27] Fleming, I. (1973). *Frontier orbitals and organic reactions*. London: Wiley.

[28] Minkin, V.I., Glukhovtsev, M.N., & Simkin, B.Y. (1994). *Aromaticity and antiaromaticity: Electronic and structural aspects*. New York: Wiley.

[29] Schleyer, P.R., & Jiao, H. (1996). What is aromaticity?. *Pure Appl. Chem*., *68*, 209-218. https://doi.org/10.1351/pac199668020209

[30] Glukhovtsev, M.N. (1997). Aromaticity today: energetic and structural criteria. *J. Chem. Educ*., *74*, 132-136. https://doi.org/10.1021/ed074p132

[31] Krygowski, T.M., Cyranski, M.K., Czarnocki, Z., Hafelinger, G., & Katritzky, A.R. (2000). Aromaticity: a theoretical concept of immense practical importance. *Tetrahedron, 56*, 1783-1796. https://doi.org/10.1016/s0040-4020(99)00979-5

[32] Schleyer, P.R. (2001). Introduction: aromaticity. *Chem. Rev*., *101*, 1115-1118. https://doi.org/10.1021/cr0103221

[33] Cyranski, M.K., Krygowski, T.M., Katritzky, A.R., & Schleyer, P.R. (2002). To what extent can aromaticity be defined uniquely?. *J. Org. Chem*., *67*, 1333-1338. https://doi.org/10.1021/jo016255s

[34] Chen, Z., Wannere, C.S., Corminboeuf, C., Puchta, R., & Schleyer, P. von R. (2005). Nucleus independent chemical shifts (NICS) as an aromaticity criterion. *Chem. Rev.*, *105*(10), 3842-3888. https://doi.org/10.1021/cr030088

[35] Gershoni-Poranne, R., & Stanger, A. (2015). Magnetic criteria of aromaticity. *Chem. Soc. Rev*., *44*(18), 6597-6615. https://doi.org/10.1039/c5cs00114e

[36] Dickens, T.K., & Mallion, R.B. (2016). Topological ring-currents in conjugated systems. *MATCH Commun. Math. Comput. Chem*., *76*, 297-356.

[37] Stanger, A. (2010). Obtaining relative induced ring currents quantitatively from NICS. *J. Org. Chem*., *75*(7), 2281-2288. https://doi.org/10.1021/jo1000753

[38] Monajjemi, M., & Mohammadian, N.T. (2015). S-NICS: An aromaticity criterion for nano molecules. *J. Comput. Theor. Nanosci*., *12*(11), 4895-4914. https://doi.org/10.1166/jctn.2015.4458

[39] Schleyer, P.R., Maerker, C., Dransfeld, A., Jiao, H., & Hommes, N.J.R.E. (1996). Nucleus independent chemical shifts: a simple and efficient aromaticity probe. *J. Am. Chem. Soc*., *118*, 6317-6318. https://doi.org/10.1021/ja960582d